https://doi.org/10.6113/TKPE.2018.23.4.265

직류 마이크로그리드에서 펄스형 부하 보상용 슈퍼커패시터 무순단 제어법

담두이헝[1], 이홍희†

A Seamless Control Method for Supercapacitor to Compensate Pulsed Load in DC Microgrid

Hung D. Dam[1] and Hong-Hee Lee†

Abstract

This paper proposes a new control method for the supercapacitor (SC) to compensate the pulsed load and to enhance the power quality of the DC microgrid. By coordinating the operating frequency, the SC is controlled to handle the surge current, while the low-frequency current component is dealt with by the remaining sources in the system. The operation mode of the SC unit is automatically changed based on the state of charge and DC bus voltage level. Meanwhile, the mismatch in the power demand is covered by the SC unit by regulating the DC bus voltage level. The effectiveness of the proposed method is verified experimentally by the prototype with two distributed generators and one SC unit.

Key words: Supercapacitors, Ultracapacitor, Pulsed load, DC microgrid

1. Introduction

Recently, the microgrids(MGs) have been increased and demand a better integration with various distributed renewable sources(RES) such as photovoltaic, wind turbine and fuel cell[1],[2]. In the past, AC MG has been employed due to the existed AC grid. However, DC MG has been concerned attractively in these days because most of RESs and the storage systems are inherently DC sources, and it is convenient and efficient for integrating the RESs and the storage systems.

Fig. 265 illustrates the typical configuration of a DC MG composed of various RESs and the energy storage system(ESS). Each unit is connected to a common DC bus via a DC-DC converter or AC-DC converter. In the microgrid systems, ESS plays an important role in DC MGs such as supporting a transient high-power and dispatching the fluctuating power of RES[3]. For instance, the pulse current causes a significant increase in the operation temperature of Li-ion batteries, which would reduce the system efficiency and make the battery lifetime

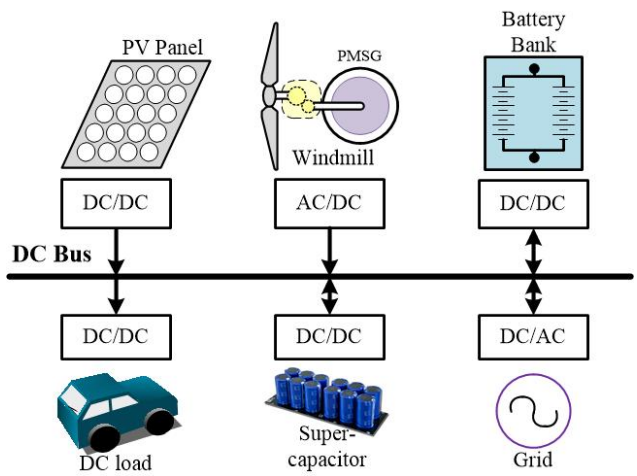

Fig. 1. Typical configuration of DC microgrid.

Paper number: KIPE-2018-23-4-5
Print ISSN: 1229-2214 Online ISSN: 2288-6281
† Corresponding author: hhlee@mail.ulsan.ac.kr, School of Electrical Eng., University of Ulsan
Tel: +82-52-259-2187 Fax: +82-52-259-1686
[1] School of Electrical Eng., University of Ulsan
Manuscript received Oct. 24, 2017; revised Nov. 28, 2017; accepted Jun. 1, 2018
— 본 논문은 2017년 전력전자학술대회 우수추천논문임
— 본 논문은 2017년 전력전자학술대회 우수논문상 수상논문임

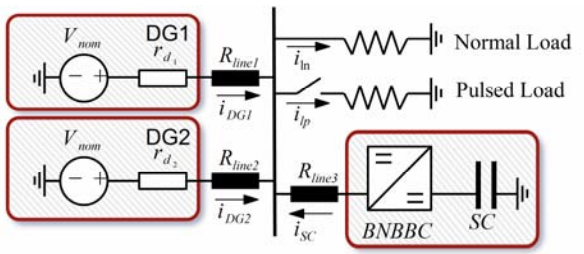

Fig. 2. Typical DC microgrid with Super-capacitor.

shorter. Furthermore, a fast load changes and the low-frequency current ripples shorten the lifetime of the fuel cell and affect its long-term performance[4]. In some applications where the load profile generates the repeated peak current, the power rating of the generator becomes higher with ESS. However, the ESS with the conventional battery cannot handle the peak current effectively which changes quickly. To solve this problem, the supercapacitor(SC) is considered to compensate the peak current due to the pulsed load or the transient load changes.

When the load changes, many researchers have focused on compensating the surge current by using dedicated topology, virtual impedance or high-pass filter method[5]-[11]. J. Cao, et al., in [5] used a dedicated topology to connect the SC and ESS. It requires less power rating for the DC-DC converter, but the DC bus voltage stability becomes worse. In [6]-[8], a high-pass filter is used to improve DC bus voltage regulation, and the ESS current can be smoothly compensated. In [9]-[11], authors used the virtual impedance methods for cooperative operation with the SC and other units. However, these methods cannot seamlessly restore the state of charge(SoC) of SC, and it needs an additional controller to regulate the SoC of SC. The controller must switch its mode from compensating mode to regulating SoC mode, so that it interrupts the operation of the SC unit.

In this paper, we propose a seamless control method that smoothly changes the operation mode and precisely controls the SC unit to compensate the transient and pulsed load currents, and also restore SoC of SC. The system design guideline is suggested, and the effectiveness of the proposed method is proved with a DC microgrid prototype.

2. System Configuration

The system considered in this paper is shown in Fig. 2. Sources and loads are connected to a common

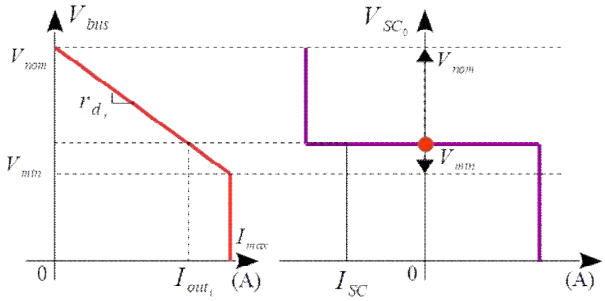

Fig. 3. DC bus voltage level based coordinated operation.

DC bus. The SC unit is used to compensate the current mismatch between the DGs' output currents (i_{DG1} and i_{DG2}) and the load current i_{load} to regulate the DC bus voltage. The SC is connected to the DC bus via Bidirectional Noninverting Buck-Boost Converter(BNBBC)[10]. From Fig. 2, the SC and load currents are

$$\begin{cases} i_{SC} = i_{load} - i_{DG1} - i_{DG2} \\ i_{load} = i_{\ln} + i_{lp} \end{cases}, \tag{1}$$

where $i_{\ln}$ and i_{lp} are the normal and the pulsed load currents. The DG converter is controlled by the droop controller, and its output voltage is expressed as

$$v_{out_i} = V_{nom} - r_{d_i} i_{out_i}, \tag{2}$$

where V_{nom} is the nominal voltage; v_{out_i} and i_{out_i} are the output voltage and the current of DG converter, respectively. The droop coefficient or the virtual resistance, r_{d_i}, is determined by the DG's rated current $i_{DG_{\max}}$, and the minimum allowable bus voltage, $V_{\min}$:

$$r_{d_i} = \frac{(V_{nom} - V_{\min})}{i_{DG_{\max}}}. \tag{3}$$

Then, DG can be modeled as a constant source V_{nom} connected serial with a resistant r_{d_i} shown in Fig. 2. Therefore, to maintain the DC bus voltage constant, it is important to supply the transient load current immediately, and it can be achieved by the SC converter. Moreover, because the DG output current is limited by its rated power, the DG cannot supply the peak current which is higher than its rated current when a pulsed load is connected to the system.

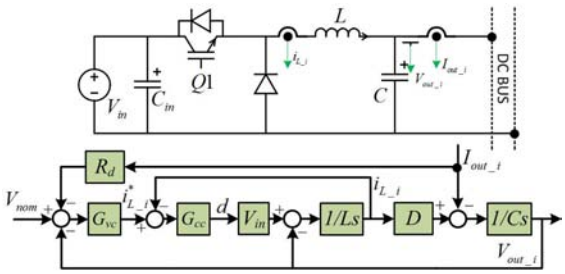

Fig. 4. Control diagram of DG converter.

3. Proposed Control Method

The DC bus voltage level is used for cooperation between DGs and SC unit in DC microgrid. The DG converter is designed to follow the DC bus voltage as given in (2). Meanwhile, the SC converter is controlled to regulate the DC bus voltage by managing the transient load current. As shown in Fig. 3, the DC bus voltage level is maintained constant by the SC converter in spite of the load variation. According to the DC bus voltage, the DGs supply the low frequency current components to the load and regulate the SoC of SC.

3.1 Droop control for DGs

The conventional droop controller is used to control the DG converter as shown in Fig. 3. The output voltage of the droop controller is expressed as

$$V_{out_i}^{*} = V_{nom} - I_{out_i} r_{d_i} \ , \tag{4}$$

where r_{d_i} and V_{out_i} are the virtual impedance of the droop controller and the output voltage of i-th DG, respectively, and V_{nom} is the nominal voltage.

DG converter is implemented by Buck converter as shown in Fig. 4, and its inner current control loop is expressed as

$$[(i_{L_i}^{*} - i_{L_i}) G_{cc}(s) V_{in} - V_{out_i}] \frac{1}{sL} = i_{L_i}. \tag{5}$$

And, the open loop and closed loop transfer function of the current controller are obtained as follows:

$$T_{CO} = V_{in} G_{cc}(s) \frac{1}{sL} \quad , \tag{6}$$
$$T_{CC} = \frac{V_{in} G_{cc}(s)}{V_{in} G_{cc}(s) + sL}$$

where the PI regulator for the current controller $G_{cc}(s)$ is given in (7):

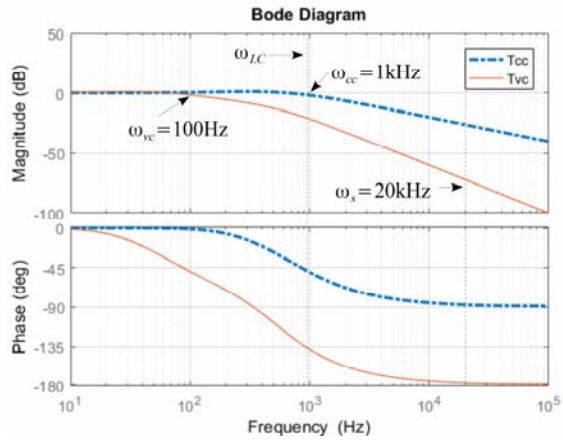

Fig. 5. Bode diagram of closed voltage and current control loop.

$$G_{cc}(s) = K_{Pc_i} + \frac{1}{s} K_{Ic_i}. \tag{7}$$

The cut-off frequency ω_{cc} of the current control loop is chosen as 1/20 switching frequency ω_s.

The voltage control loop is represented as

$$[(V_{nom} - V_{out_i} - i_{out_i} R_d) \quad . \tag{8}$$
$$\times G_{vc}(s) T_{cc}(s) D - I_{out_i}] \frac{1}{Cs} = V_{out_i}$$

From (4), the voltage control loop in (8) becomes

$$[(V_{out_i}^{*} - V_{out_i}) \quad . \tag{9}$$
$$\times G_{vc}(s) T_{cc}(s) D - I_{out_i}] \frac{1}{Cs} = V_{out_i}$$

Then, the open loop and closed loop transfer function of the voltage controller are given in (10):

$$T_{VO} = G_{vc}(s) T_{CC}(s) \frac{D}{Cs} \tag{10}$$
$$T_{VC} = \frac{G_{vc}(s) T_{CC}(s) D}{G_{vc}(s) T_{CC}(s) D + Cs}$$

The cut-off frequency of the voltage control loop ω_{vc} is chosen as 1/10 ω_{cc}. Fig. 5 shows the bode diagram of the designed controller. It shows that the cut-off frequencies of voltage and current loops are designed accurately.

3.2 Controller for Supercapacitor

As shown in Fig. 6, the SC unit converter is implemented by bidirectional non-inverting buck-boost converter(BNBBC), which is controlled by the dual-carrier modulator[12]. The parameters of the SC converter are shown in table I. The duty cycles d_1

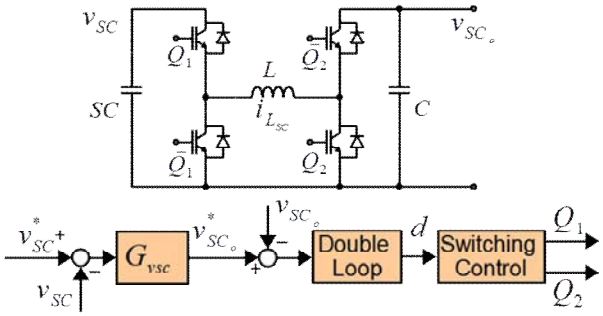

Fig. 6. Control diagram of SC converter.

TABLE I
SC CONVERTER PARAMETERS

Parameters	Symbol	Value
Super-capacitor	$C_{SC}, V_{SC_{max}}$	66F, 48V
SC normal voltage	V_{SC}	40V
Mode threshold[12]	V_H , V_L	0.5,-0.5
Switching frequency	f_s	20kHz
Inductor	L	0.5mH
Output capacitor	C	4400uF

and d_2 for the switches Q1 and Q2 in Fig. 6 are calculated as following:

$$d_1 = \begin{cases} 0, & d \le -1 \\ K_H(1+d), & -1 \le d \le V_H, \\ 1, & d \ge V_H \end{cases} \qquad (11)$$
$$d_2 = \begin{cases} 0, & d \le V_L \\ K_L(d-V_L), & V_L \le d \le 1 \\ 1, & d \ge 1 \end{cases}$$

where $K_H = (1+V_H)^{-1}$, $K_L = (1-V_L)^{-1}$ and d is output control signal from the double loop controller.

From the proposed control block diagram in Fig. 6, there are three control loops: SC voltage loop, output voltage loop and current loop. The SC voltage control loop regulates the SC voltage v_{SC} to be the desired voltage, and generates the output voltage reference $v^*_{SC_o}$. Based on the SC voltage level, the SC voltage loop decides the operation mode of SC converter by the output voltage reference value. After that, the output voltage of the SC converter is controlled by a double loop voltage-current controller.

3.2.1 Inner current loop

The inner current control loop is shown in Fig. 7. By using the small signal analysis in [12], the relationship between the inductor current and the duty cycle in the Laplace domain is expressed as

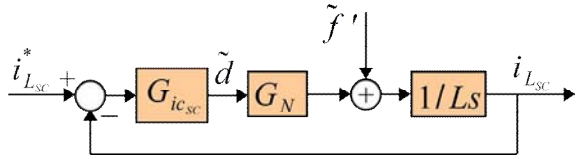

Fig. 7. Inner current control diagram.

$$\widetilde{i_{L_{SC}}}(s) = \frac{1}{Ls}(G_N\tilde{d}(s) + \widetilde{f'}(s)), \qquad (12)$$

where

$$G_N = \frac{2}{3}(K_H V_{SC} + K_L V_{nom}). \qquad (13)$$

The transfer function between the control signal and the inductor current is obtained by assuming $\widetilde{f'}(s) = 0$:

$$\left.\frac{\widetilde{i_{L_{SC}}}}{\tilde{d}}(s)\right|_{\widetilde{f'}(s)=0} = \frac{G_N}{Ls}. \qquad (14)$$

Then, the open loop current transfer function becomes

$$T_{iL_{open}}(s) = G_{ic_{SC}}(s)\frac{G_N}{Ls}, \qquad (15)$$

where the compensator $G_{ic_{SC}}(s)$ means a PI controller and it is given as

$$G_{ic_{SC}}(s) = K_{Pic\ SC} + \frac{K_{Iic_{SC}}}{s}. \qquad (16)$$

The gains $K_{Pic\ SC}$, $K_{Iic_{SC}}$ of $G_{ic_{SC}}(s)$ are chosen under the constraint that the cut-off frequency of $T_{iL_{open}}(s)$ is 1/20 switching frequency ω_s. Because of the symmetrical configuration of the converter legs in Fig. 6, the current loop uses same current compensator gains for both power flow directions.

3.2.2 Output voltage control loop

The output voltage control loop, which is slower than the inner current loop, has 1/10 cut-off frequency of the inner current loop. The outer voltage loop is shown in Fig. 8. The open loop transfer function of the outer voltage loop is given as

$$T_{vo_{open}} = G_{vc_{SC}}(s)T_{iL_{closed}}(s)\frac{1}{Cs}, \qquad (17)$$

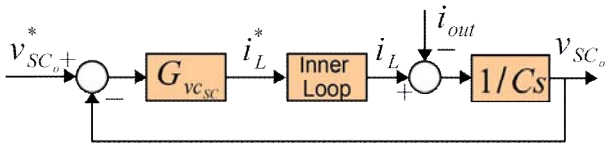

Fig. 8. Outer voltage control diagram.

where $G_{vc_{SC}}(s)$ in (18) is a PI controller for the voltage compensator,

$$G_{vc_{SC}}(s) = K_{Pvc_{SC}} + \frac{K_{Ivc_{SC}}}{s} \tag{18}$$

$T_{iL_{closed}}(s)$ is the closed loop transfer function of the inner current loop, and C is the output capacitor of the SC converter. When the inner loop is designed stably, the outer voltage loop is designed with an assumption of $T_{iL_{closed}} \approx 1$. Hence, the open loop of the outer voltage controller can be rewritten as following:

$$T_{vo_{open}} = G_{vc_{SC}}(s)\frac{1}{Cs}. \tag{19}$$

Then, the gains $K_{Pvc_{SC}}, K_{Ivc_{SC}}$ of $G_{vc_{SC}}(s)$ are determined under the constraint that the cut-off frequency of outer voltage control loop $T_{vo_{open}}(s)$ is 1/10 of the inner current loop.

The bode diagram of inner double loop is shown in Fig. 9. It shows that the cut-off frequency of the current and voltage loop are to meet the design requirements.

3.2.3 SC voltage control loop

The SoC of the SC is simply calculated in (20):

$$SoC = \frac{V_{SC}^2 - V_{SC_{\min}}^2}{V_{SC_{\max}}^2 - V_{SC_{\min}}^2}, \tag{20}$$

where V_{SC} is the output voltage of the SC, $V_{SC_{\max}}$ and $V_{SC_{\min}}$ are the maximum and minimum allowable output voltage of the SC, respectively. In order to restore the SoC of the SC, the SC voltage should be regulated around its rated value. For this purpose, the SC voltage is controlled by the SC voltage control loop. When the SC needs to be charged, the output voltage of the SC converter is controlled to reduce its magnitude, and the power flows from the DGs to the

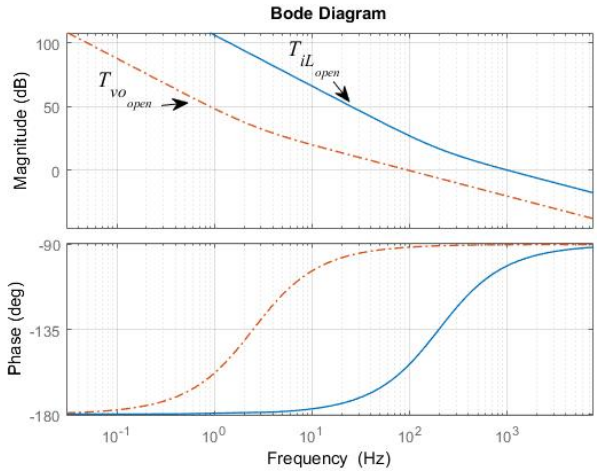

Fig. 9. SC voltage control diagram.

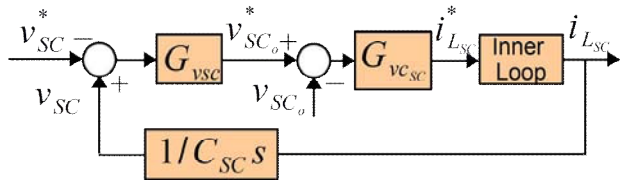

Fig. 10. SC voltage control diagram.

SC. On the other hand, the output voltage of the SC converter is controlled to increase its magnitude when the SC needs to be discharged, and the power flows from the SC to the DC bus. As a result, the Sc converter smoothly switches its operation modes without any mode switch and interruption in control loop.

The open loop transfer function of SC voltage controller is expressed in (21) from Fig. 10:

$$T_{vsc_{open}} = G_{vsc}(s)G_{vc}(s)\frac{1}{C_{SC}s}, \tag{21}$$

where $G_{vsc}(s)$ is a PI controller and it is given in (22), and C_{SC} is the capacity of SC.

$$G_{vsc}(s) = K_{Pvsc} + \frac{K_{Ivsc}}{s}. \tag{22}$$

In this paper, the cut-off frequency of $T_{vsc_{open}}$, ω_{sc}, is chosen to be $0.1Hz$, and the PI controller gains K_{Pvsc}, K_{Ivsc} of $G_{vsc}(s)$ are obtained to satisfy (22):

$$\left| T_{vsc_{open}} \right|_{s=j\omega_{sc}} = 1. \tag{23}$$

To verify the stability of the control loop, the root locus is plotted in Fig. 11 by changing the SC capacity.

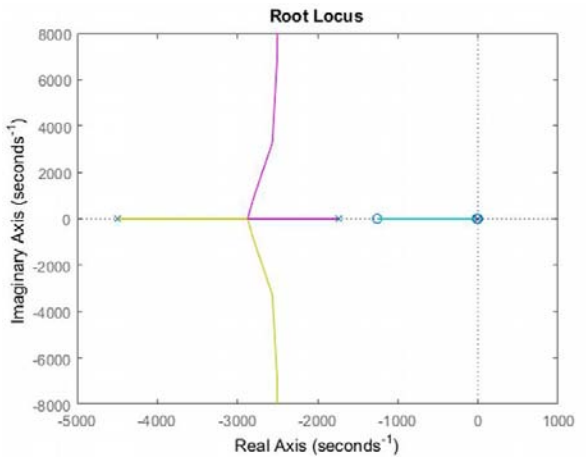

Fig. 11. Root locus plots of SC voltage loop control.

TABLE II
DC MICROGRID PARAMETERS

Parameters	Symbol	Value
Bus voltage	V_{min}–V_{nom}	45–48V
Line impedance	r_{line}	0.05 ohm
Super-capacitor		66F, 48V
SC normal voltage		40V
pulsed loads		5 ohm, 3.5 ohm
Normal load		10 ohm
Rated current of DGs	I_{rated}	5A
Droop coefficient	r_{d1},r_{d2}	0.6

As we can see, all poles and zeros are located on the left hand plane, and the control loop is stable regardless of the SC capacity variation.

4. Experimental Results

The prototype for DC mocrogrid system in Fig. 2. is implemented, and the system parameters are given in Table II. Two DG converters are controlled by single TMS320F28335 DSP controller; another DSP controller is used for the SC unit converter. In order to evaluate the proposed method, two cases are studied: Case I shows the normal operation of the proposed method; Case II shows the performance of the proposed method when the DG's output power changes.

4.1 Case I:

Two DGs are controlled by the droop controller to share the load current, while the SC is controlled to regulate the DC bus voltage by compensating the pulsed load current. The pulsed loads is sequentially connected to the DC bus as shown in Fig. 12. It shows

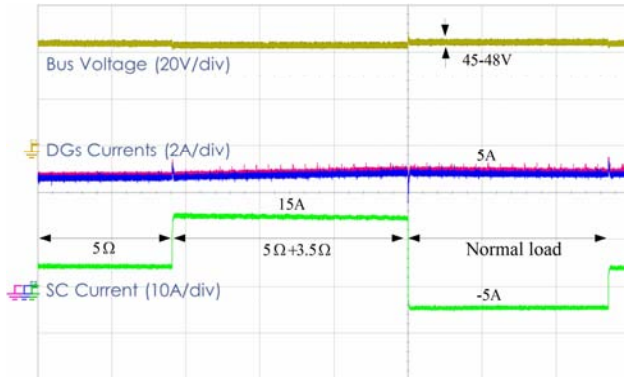

Fig. 12. Case I: The output current of SC and DGs when pulsed loads are connected (2s/div).

that the output currents of DG1 and DG2 are kept constant at 5A regardless of the changes of the pulsed loads because the SC unit handles the peak current against the pulsed load. And also, the DC bus voltage is constantly regulated within the allowable voltage variation from 45V to 48V.

4.2 Case II:

To investigate the performance against the current disturbance due to the power variation of the renewable source, DG1 operates as a current source to inject the current of 4.5+2.5sin(100πt) A, while DG2 is controlled by the droop controller. In Fig. 13, because the output voltage of the SC is lower than the normal voltage (40V), the SC unit is controlled in charge mode. In contrast, the SC unit is controlled in discharge mode when the SC voltage is higher than 40V. From Figs. 13 and 14, it is clear that the SC effectively regulates the DC bus voltage in spite of the current fluctuation.

Fig. 15 shows the performance of the proposed method when the DG1 switches the control mode from the droop control to the current control mode. Even though the output current of DG1 is fluctuated due to the change of output power, the SC converter quickly regulates the DC bus voltage by absorbing the DG1 fluctuating current effectively. Because DC bus voltage variation directly affects the cooperation between the DG units in the microgrid, the system stability is enhanced. by reducing the DC bus voltage variation.

The experimental results show that the proposed method is effectively compensate the DC bus voltage regardless of the system disturbances, and it increases the stability due to accurate voltage regulation by menas of the SC.

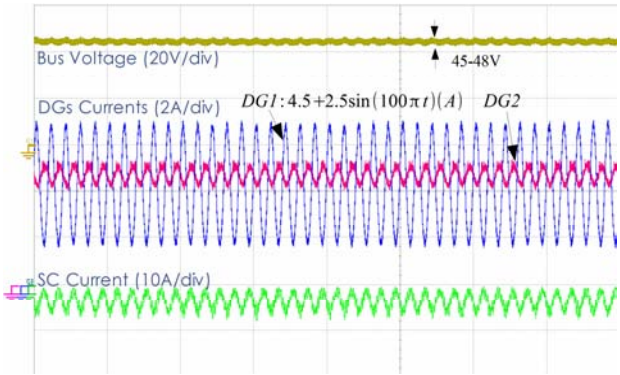

Fig. 13. Case II: SC in charge mode when DG1 inject harmonic current.

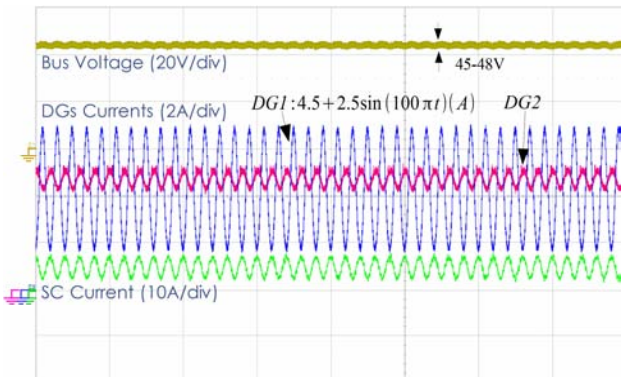

Fig. 14. Case II: SC in discharge mode when DG1 inject harmonic current.

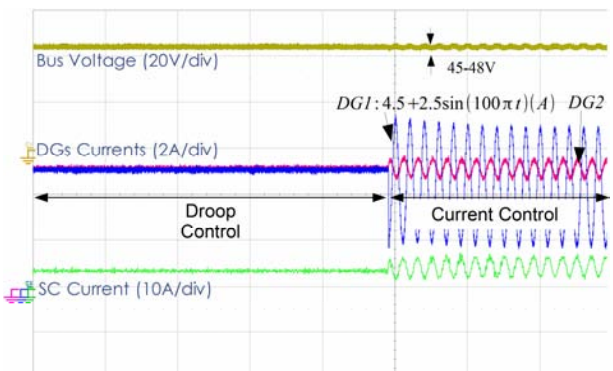

Fig. 15. Case II: when DG1 changes its output power.

5. Conclusion

In this paper, a seamless control method is proposed to compensate the surge current caused by the pulsed load by means of the SC in DC microgrid. Based on the SoC of SC, the DC bus voltage level is smoothly regulated by charging and discharging the SC. Therefore, all the disturbance current and the pulsed load changes, which cause the fluctuation of DC bus voltage, are compensated by the SC unit. The design procedure of the controller and the stability analysis are carried out and the experimental result shows the effectiveness of the proposed method.

This work was supported by the National Research Foundation of Korea Grant funded by the Korean Government(NRF-2015R1D1A1A09058166) and partly by the Korea Institute of Energy Technology Evaluation and Planning(KETEP) and the Ministry of Trade, Industry & Energy(MOTIE) of the Republic of Korea(No. 20174030201490).

References

[1] R. H. Lasseter, *et al.*, "White paper on integration of distributed energy resources, the CERTS microgrid concept," *Consort. Electr. Reliab. Technol. Solut. Gray, Davis, Gov.*, pp. 1-27, Oct. 2003.

[2] M. Barnes, *et al.*, "Real-world microgrids-an overview," in *System of Systems Engineering, 2007. SoSE'07. IEEE International Conference on*, pp. 1-8, 2007.

[3] V. A. Boicea, "Energy storage technologies: the past and the present," *Proceedings of the IEEE*, Vol. 102, No. 11, pp. 1777-1794, Nov. 2014.

[4] S. T. Hung, D. C. Hopkins, and C. R. Mosling, "Extension of battery life via charge equalization control," *IEEE Trans. Ind. Electron.*, Vol. 40, No. 1, pp. 96-104, Feb. 1993.

[5] J. Cao and A. Emadi, "A new battery/ultracapacitor hybrid energy storage system for electric, hybrid, and plug-in hybrid electric vehicles," *IEEE Trans. Power Electron.*, Vol. 27, No. 1, pp. 122-132, 2012.

[6] S. K. Kollimalla, M. K. Mishra, A. Ukil, and H. B. Gooi, "DC grid voltage regulation using new HESS control strategy," *IEEE Transactions on Sustainable Energy*, Vol. 8, No. 2, pp. 772-781, Apr. 2017.

[7] M. Hamzeh, M. Ghafouri, H. Karimi, K. Sheshyekani, and J. M. Guerrero, "Power oscillations damping in DC microgrids," *IEEE Trans. Energy Convers.*, Vol. 31, No. 3, pp. 970-980, Sep. 2016.

[8] V. Yuhimenko, C. Lerman, and A. Kuperman, "DC active power filter-based hybrid energy source for pulsed power loads," *IEEE J. Emerg. Sel. Top. Power Electron.*, Vol. 3, No. 4, pp. 1001-1010, 2015.

[9] Y. Zhang and Y. Li, "Energy management strategy for supercapacitor in autonomous DC microgrid using virtual impedance," in *IEEE Applied Power Electronics Conference and Exposition (APEC)*, pp. 725-730, 2015.

[10] Y. Gu, W. Li, and X. He, "Frequency-coordinating

virtual impedance for autonomous power management of DC microgrid," *IEEE Trans. Power Electron.*, Vol. 30, No. 4, pp. 2328-2337, Apr. 2015.

[11] X. Zhao, X. Wu, Y. Li, and H. Tian, "Energy management strategy of multiple supercapacitors in an autonomous DC microgrid using adaptive virtual impedance," in *2016 IEEE 7th International Symposium on Power Electronics for Distributed Generation Systems (PEDG)*, pp. 1-8, 2016.

[12] I. Aharon, A. Kuperman, and D. Shmilovitz, "Analysis of dual-carrier modulator for bidirectional noninverting buck-boost converter," *IEEE Trans. Power Electron.*, Vol. 30, No. 2, pp. 840-848, 2015.

Hung D. Dam

He was born in Thanh Hoa, Vietnam, in 1989. He received the B.S. degree Electrical Engineering from the Ho Chi Minh City University of Technology, Ho Chi Minh City, Vietnam, in 2012. Currently, he is an M.S./Ph.D. combined student at the University of Ulsan, Ulsan, Korea.

Hong-Hee Lee

He is a professor in the School of Electrical Engineering, University of Ulsan, Ulsan, Korea. He is also the Director of the Network-based Automation Research Center(NARC). He received his B.S., M.S., and Ph.D. in Electrical Engineering from Seoul National University, Seoul, Korea, in 1980, 1982, and 1990, respectively. He is a Senior Member of the Institute of Electrical and Electronics Engineers(IEEE), and a Life Member of the Korean Institute of Power Electronics(KIPE) and the Korean Institute of Electrical Engineers(KIEE). He is also a Senior Member of the Institute of Control, Robotics and Systems(ICROS).